Al-Azhar Bulletin of Science Vol. 31, No. 1, (June) 2020, pp. 1-9

PREPARATION AND ELECTROCHEMICAL BEHAVIOR OF THE ACTIVATED CARBON FROM POMEGRANATE PEELS AS ENERGY-STORAGE MATERIALS.

M. M. Morad[1*], Sayed Y. Attia[2],Saad G. Mohamed[2], M.M. Moharam[3],R.M. AbouShahba[1] and M.M. Rashad[3]

[1]*Chemistry Department, Faculty of Science (Girls), Al-Azhar University, Egypt.*
[2]*Chemical Engineering Department, Tabbin Institute for Metallurgical Studies, (TIMS), Helwan, Cairo, Egypt.*
[3]*Central Metallurgical Research& Development Institute (CMRDI), Helwan, Cairo, Egypt.*
*Corresponding Author ;E-mail: monyam19@yahoo.com

ABSTRACT

This study investigates the electrochemical evaluation of the activated carbon (AC) prepared from pomegranate peels which were collected, dried, carbonized and finally activated with KOH at different temperatures. The characterization of the as-prepared AC revealed an amorphous type of carbon and densely layer-stacking sheets with an interconnected micro porous network with a remarkable 3128.86m^2g^{-1} surface area. The as-synthesized AC displayed a remarkable capacitance of 126 F g^{-1} at 0.5 A $g^{-1}$with a storage retention of 137 % after 2000 cycles at a current density of 2 A g^{-1}. Meanwhile, the realistic symmetrical simulation has been installed, it shows an energy density of 4.58 W h kg^{-1} at a power density of 244 W kg^{-1} with a storage retention of 66 % of the initial capacity at a current density of 2 A g^{-1} after 2000 cycles. Overall, these results demonstrate that for supercapacitors evaluation, the AC electrode can be considered a successful electrode material.

Keywords: Activated carbon; Pomegranate peels; Supercapacitors; Symmetric device; Energy storage.

1. INTRODUCTION

Efforts to deplete the environmental impacts accompanying greenhouse gas emissions have boosted universal demands in growing sustainable energy-sources worldwide[1-3].Renewable sources of energy include solar and hydropower which are the most auspicious solutions to these problems[4-8]. As a result of the great instabilities in the electricity generated from renewable energy resources, it is essential to be stored effectively to provide the demanded-energy [9-11]. Batteries and supercapacitors (SCs) are the prime technologies for electrochemical energy-storage energy-storage amongst the different energy-storage systems. SCs based on rapid electrostatic processes or Faradaic-electrochemical routes. The charge is mostly stored at the electrode (active material) /electrolyte interface, such as high surface area porous carbonaceous materials, metal compounds, or conductive polymers. Though the storage of charges and performance origins are analogous to the traditional capacitors, the specified capacity and specific energy in the SC increase by 100,000 or larger than the conventional ones, which can be achieved by introducing active-electrode materials with surface areas of 1000 times higher, nanoscale spaces, and further pseudocapacitance by rapid Faradaic reactions. Consequently, SCs store thousands of Farads in one device, much higher than that are stored by conventional capacitors. SCs feature batteries in which SCs can provide rapid charge/discharge times (seconds to minutes), but with reduced specific energy. In addition to high power density, SCs further possess some other benefits over batteries, such as operational safety, long-life of cycling, extraordinary efficiency, and high stability [12].

In general, SCs electrodes can be categorized into three dissimilar models including electric-double layer capacitors (EDLCs), pseudocapacitors, and battery-type capacitors[13]. Consequently, asymmetric SCs devices are constructed from two capacitive-type electrodes [14-18]and hybrid SCs devices which are constructed from two electrodes, one can store the charge by a faradaic battery-type process whereas the other electrode employs a capacitive mechanism for charge-storage[19-23].

Activated carbon (AC) has been widely recognized as SC electrode material, whose unique physical and chemical properties, excellent conductivity, low cost, and high surface area are considered [23-26]. AC has been developed from various biomass sources, for instance, banana fibers, Argan seed shells, corn grains, camellia oleifera shell, oil palm, sugarcane bagasse, scrap waste tires, and onion dry peel waste [27-32]. ACis classified as EDLCs, where energy can be stored in the electrolyte/electrolyte double-layer interface, it also has enticed considerable attention despite the high density of energy, long life and fast charging capacity[33-35].

In this work, the main objective is to prepare the AC from low-cost pomegranate peels and the study of its electrochemical performance in an electrolyte solution with 6 M KOH. The as-prepared AC is an amorphous carbon with densely layered sheets with a porous network interconnected, AC with a microporous characteristic was found to give a very high surface area of 3128.86 m^2 g^{-1}. The as-synthesized material exhibited a good electrochemical performance at 0.5 A g^{-1} with a remarkable capacitance of 126 F $g^{-1}$and superior cycling stability of 137% capacitance retention at 2 A g^{-1} after 2000 cycles.

2. EXPERIMENTAL SECTION

2.1 Preparation of AC from pomegranate peels

The pomegranate peels were firstly washed with deionized water and dried at 105°C. The carbonization process was implemented at 850°C for 2h with a heating rate of 5°C min^{-1}, accompanied by room temperature cooling. The carbonized sample was crushed with a 4-fold weight of KOH, as an optimum ratio which increases the yield and surface area [36-38],using a ball mill at speed 400 rpm for 40 min for well mixing. The mixture was heated in a tubular horizontal furnace at different temperatures and times. Firstly, the mixture was heated at 200°C for 60 min with 150 ml/min of nitrogen flow, the sample temperature was raised to 500°C for 60 min, and then also raised to 850°C for 100 min with a 5 °C/min heating rate[38].After cooling down to room temperature, the residue was repeatedly washed with water and ethanol, then collected by filtration to get the prepared black AC from Pomegranate peels. The synthesis of AC was repeated three times to approve the reproducibility of the results.

2.2 Characterization of the materials

The powder X-ray diffraction (XRD) (Brucker D8 diffractometer) was used to characterize the purity and crystallinity of the as-prepared AC using the Cu-Kα (λ=1.5406A^0) radiation in the range 2θ from 10^0 to 70^0 and scanning rate of 20 min^{-1}. The morphologies were studied using a JEOL instrument (JSM – 5410, Japan), using field emission scanning electron microscopy (FSEM).The chemical composition of the AC was determined using X-ray photoelectron spectroscopy (XPS, scientific thermos) using Al Kα monochromatized radiation. A JY Lab-Ram HR800 Raman spectrometer was used to collect Raman spectrum. The actual surface area was measured using the Brunauer – Emmett – Teller (BET, Quanta chrome NovaWin) process.

2.3 Electrochemical characterization

The as-prepared AC electrode performance was electrochemically evaluated in 6 M KOH solution as the electrolyte via 3-electrode system. AC was combined with carbon black and Nafion (as a binder) for working electrode manufacturing in a weight ratio of 80:10:10,

respectively, to create a suspended solution, 0.5 mL of ethanol was added into the mixture. Drop-casting the suspended solution onto a piece of nickel foam (1 cm x 3 cm) substrate (NF, 1.6 mm thickness, Xiamen Tob New Energy Technology Co. LTD, China) installed the working electrode. The casted-film was then overnight dried at 70°C. The electrochemical behavior of prepared AC electrode was investigated at room temperature by (Volta lab 40 PGZ 301, Radiometer Analytical, France) with a platinum wire as a counter-electrode and a saturated calomel electrode (SCE) as a reference electrode. The symmetric system was designed for a practical application, in which the as-prepared AC was tested as a positive and negative electrode (denoted as AC//AC).

Cyclic voltammetry (CV) measurements were tested at various scanning rates from 10 to 50 mV s^{-1} in a potential range of -1 to 0V (vs SCE). Within a potential range of -1 to 0 V (vs SCE), galvanostatic charge/discharge (GCD) was performed at varying current densities from 0.5 to 3 A g^{-1}. The Electrochemical impedance spectroscopy (EIS) measurements were analyzed using Nyquist plots in the frequency range 100 kHz to 0.01 Hz. At current density of 2 A g^{-1} the stability experiment was evaluated. From the GCD results the specific capacitance (Csp) F g^{-1} was estimated according to the following equation [39, 40].

$$C_{sp} = I\Delta t / m\Delta V \quad (1)$$

Where I is the current applied in GCD test (A), Δt is the time of discharge (s), ΔV is the potential window (V) and m is the active material mass (g).

3. RESULTS AND DISCUSSION

3.1 AC characterization.

Fig. 1a displays XRD result of the prepared AC, there are no observed peaks in the pattern, indicating the amorphous nature of the AC. The Raman analysis as shown in fig. 1b, investigated the graphitization degree for the AC sample. The D and G bands, respectively, are two wide peaks located at 1333 and 1575 cm^{-1} for AC. The D band represents the defects and the carbon material disorder (A1 g symmetry) while the G band is associated with the bond stretching of the sp2 carbon atoms pair (E2g symmetry). The graphitization degrees and defects are illustrated from the ID / IG intensity ratio.

For example, the intensity ratio (1.03) which implies the high structural defects in AC could be due to KOH activation may produce defects and nanopores in the carbon frameworks. Subsequently, as the amount of KOH increases, the degree of graphitization decreases(larger ID / IG ratio). The larger ID / IG values (1.03) may increase defects that act as the active and adsorption sites, thus enhancing SCs performance and catalytic activity[41, 42].

Fig. 1c and d describe XPS analysis, which shows different surface atoms compositions for the sample. The centered peaks of 285 and 532 eV refer to C1s and O1s, respectively [43,44]. Fig.1c. confirms the high resolution C1s spectra of AC. C1scan be deconvoluted into four spectral components indexed by (C=C), (C–C),(C–O), and carboxyl/epoxy (O-C=O) at binding energies of 284.4, 284.4 285.4 eV, respectively [45-47].In particular, AC high-resolution XPS spectra of O1s (Fig. 1d) was deconvoluted to three peaks at binding energies of 531.7, 530.7, and 532.3 eV, signifying the presence of C-OH, C–O, and O–C=O group srespectively [48].

Fig. 2a and b show the as-prepared AC isotherm of the nitrogen adsorption/desorption. At the activation temperature of 850 ° C, the calculated BET surface area of the AC from the isotherm in the P/P_0 range of 0.01 to 0.1 is 3128.865 m^2 g^{-1}.This BET surface area value is similar to that of AC made from biomass resources (3164 m^2 g^{-1})[49]. The BET curve displays the standard type I isotherms as illustrated by the IUPAC classification[50],

specifying the microporous feature of this AC sample. The total volume of the active carbon pores was calculated using the amount of nitrogen adsorption at the P/P_0 value of 0.98718 is 1.87 $mlg^{-1}$with an average pore diameter of 2.2 nm. Surface morphology of AC from pomegranate peels (Fig. 3a) is evinced in Fig. 3b,c, and d (SEM images), displaying densely stacked-layers of the carbon sheets with a porous network interconnected to them.

3.2 Electrochemical properties of the AC electrode

The CV as well as GCD and EIS were measured in 6 M KOH to estimate the electrochemical properties of the prepared activated carbon as an active electrode material for SCs, as seen in the fig. 4. Plainly, Fig. 4a indicates that the CV curves (at varying scan rates from 10 to 50 mV s^{-1}) of the prepared AC in which at low scan-exhibit a semi-rectangular shape and a deviated oval-like shape at a high scan rate in the potential range from -1 to 0V without any faradaic redox peaks at all scanning rates. This illustrates the ideal EDLC behavior of the prepared electrode and the absence of pseudo-capacitance effect, in which energy storage systems collect energy at the double layer interphase of the electrode /electrolyte [51, 52].

In Fig. 4b, the GCD tests of the prepared electrode were conducted for further investigation of the electrochemical performance. Clearly, GCD curves present linear and symmetric charge / discharge curves at different current densities from 0.5 to 3 A g^{-1} with the same potential window (-1 to 0 V). The specific capacitance as a function of current density of AC electrode can be determined from GCD, Fig. 4b, using equation 1. AC manifests a high specified capacitance value of 126 F g^{-1} at 0.5 A g^{-1} higher than that reported before such as honeycomb AC from agriculture waste (76 F g^{-1} at 0.025 A g^{-1}), Allium cepa (onion dry peel waste, 189.4 at 0.1 A g^{-1}) [27,32], AC obtained from Amygdalus pedunculata shell (50 F g^{-1})[38], and AC nanofibers (150 F g^{-1} at 10 m A g^{-1})[53].

Cycling life was achieved using GCD measurements. The stability test of the prepared AC electrode was demonstrated at 2 A g^{-1} for 2000 cycles as shown in Fig. 4c.AC electrode exhibited a notable cycling stability after 2000 cycles (137% capacitance retention). The improvement of capacitance during long cycling could also be due to the activation influence throughout the electrochemical cycling, the increase in wetting of electrode surface with cycling, and the electrolyte ions diffusion into the newly opened microporous on the electrode by cycling, resulting in an increase in the electroactive surface area. [54].

At open-circuit voltage, Nyquist plots show EIS of the prepared active carbon being obtained in Fig.4d. The intersection of the graph at the real part (Zr) in the high-frequency area describes the equivalent series resistance (ESR), Which is linked to the ionic resistance of the electrolyte, internal resistance of the active material electrode and contact resistance of the electrode with the current collector [55]. From the plots, AC as a fresh electrode has a similar value of ESR (3.2 ohm) to that after a stability test (3 ohm), suggesting the absence of an Ohmic loss during cycling due to the high conductivity of the AC electrodes. The Nyquist plots show a low frequency semicircle and a near vertical line in the high frequency region. In the low frequency area the near-vertical line indicates that AC electrode exhibited better capacitive behavior.

3.3 Electrochemical performance of the symmetric SC.

To estimate the electrochemical efficiency of the AC electrode for practical application in a two-electrode cell configuration. The EDLC symmetric device was assembled in an electrolyte of 6 M KOH using two electrodes of the prepared AC, one electrode as a positive part and the other as a negative one(presented as AC//AC) within an operating voltage of 0.0 to 1.0 V. The CV curves of the AC//AC device are shown in Fig. 5a at different scan rates from 10 to 100 mV s^{-1} over a potential range of 0.0 to 1.0 V. All CV curves of the symmetrical SC

present the near-rectangular CV shapes without any faradaic redox peaks at all scan rates. This reveals the ideal EDLC behavior for both electrodes and the absence of a pseudocapacitance effect. As manifested in Fig.5b,GCDtested at various current densities of 0.5, 1, 2, 3, 4, 5 and 10 A g^{-1}, However, the linear charging / discharge profile confirms the lack of Faradic-type of AC/AC, AC//AC EDLC system shows a specific capacitance value of 33 F g^{-1} at 0.5 A g^{-1}, Ed at 4.58 Wh kg^{-1}, and Pd at 248 W kg^{-1}.

The as-fabricated device's cycling stability was achieved by running the GCD test at a current density of 2 A g^{-1} within 0 to 1 V, as illustrated in Fig. 5c. The AC//AC system exhibited 66 % capacity retention after 2000 cycles of the first cycle capacitance value, showing the EDLC device's worthy reversibility and stability. EIS was performed, as shown in Fig. 5d, for the AC//AC EDLC system, showing a smaller ESR (2.5 Ohm).It was observed that ESR slightly changed (3Ohm) after 2000 cycles, indicating a negligible Ohmic loss upon cycling. The relationship between Ed and Pd was defined using a Ragone plot based on the aforementioned data (Fig. 5e). Ragone plot promisingly exhibited an Ed of 4.5 Wh kg^{-1} at a Pd of 244 W kg^{-1}. Such results show that the AC//AC design as an EDLC capacitor has great potential for energy-storage systems.

CONCLUSIONS

AC was successfully elaborated from waste materials based on priceless pomegranate peels to investigate as a SC electrode. AC shows promising structural and morphological properties supporting its use for energy storage. CV and GCD indicate electrochemical double-layer capacitance. The AC electrode depicts a high defined capacitance value of 126 F g^{-1} at 0.5 A g^{-1}, Cycling stability of prepared AC is reached with a good capability retention of 137 %, even after 2000 cycles. The practical symmetrical AC//AC SC device was assembled, the ECDL device exhibited an E_d of 4.58 Wh $kg^{-1}$and a P_d of 244W kg^{-1}. Eventually, results show that the AC//AC system as an EDLC capacitor has great potential for applications of energy-storage devices.

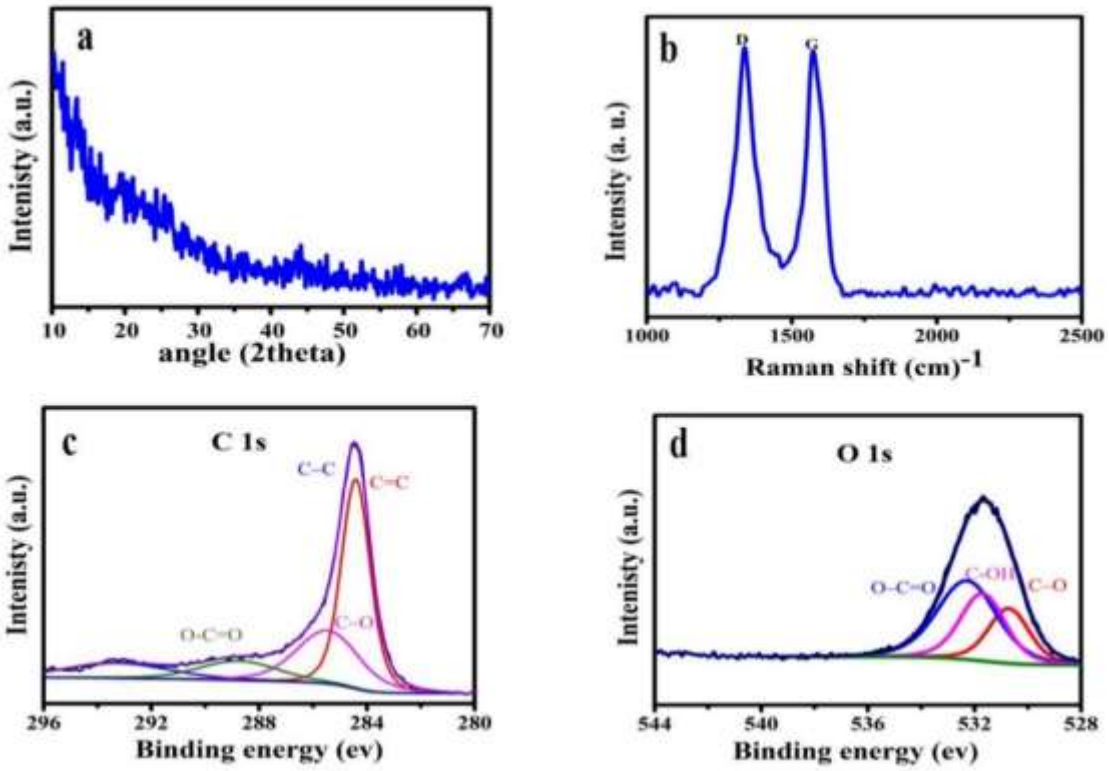

Figure 1: (a) XRD chart, (b) Raman spectrum, and (c, d) AC XPS spectrum high resolution.

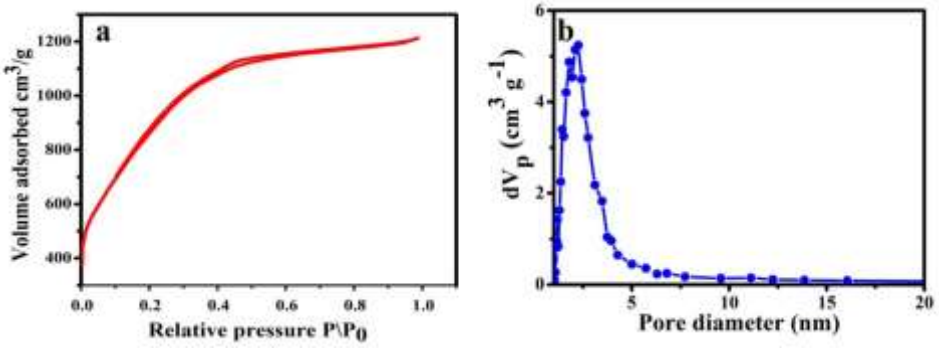

Figure 2(a) N2 isothermic adsorption – desorption and (b) distributions of AC pore size.

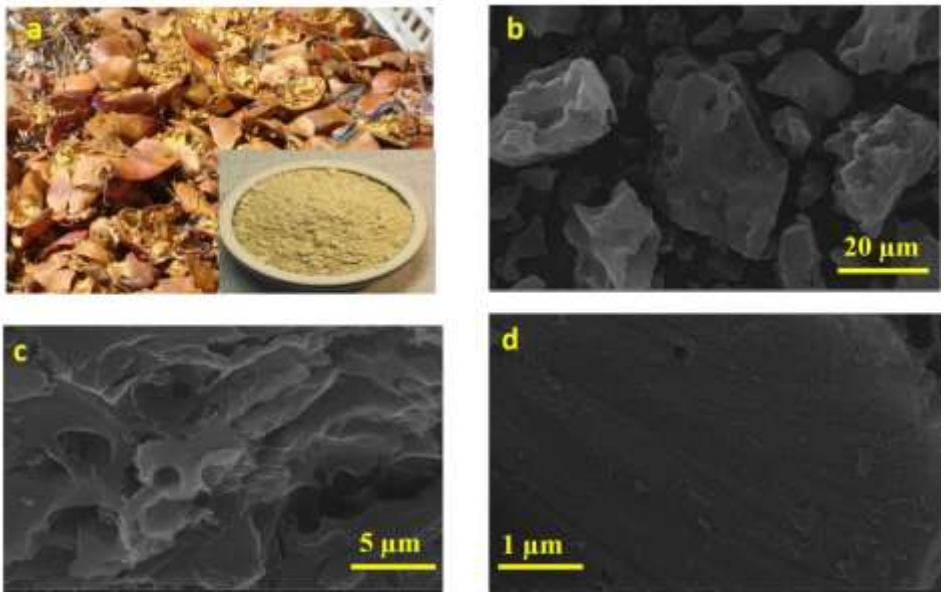

Figure 3: a) Pomegranate peels and (b), (c), (d) as-prepared AC FE-SEM images with different magnifications .

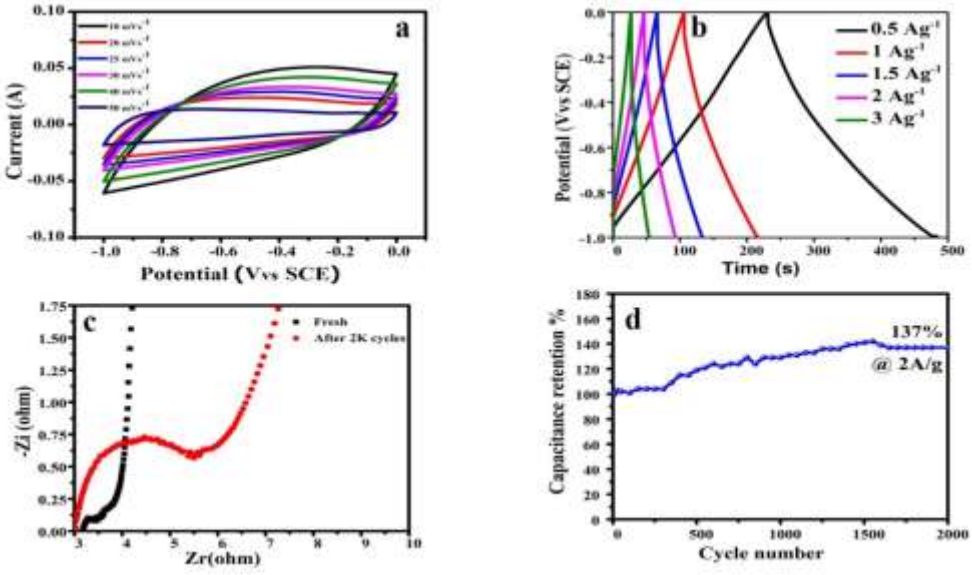

Figure 4(a) CV curves at different scanning rates from 10 to 50 mV s^{-1}(b) GCD at variable current densities from 0.5 to 3 Ag^{-1}(c) stability test at 2 A g^{-1} and (d) AC electrode EIS profile.

REFERENCES

[1]. Lashof, D.A. and D.R. Ahuja, *Relative contributions of greenhouse gas emissions to global warming.* Nature, 1990. **344**(6266): p. 529.

[2]. Chu, S. and A. Majumdar, *Opportunities and challenges for a sustainable energy future.* nature, 2012. **488**(7411): p. 294.

[3]. Nocera, D.G., *Living healthy on a dying planet.* Chemical Society Reviews, 2009. **38**(1): p. 13-15.

[4]. Hagfeldt, A., G. Boschloo, and L. Sun, *kloo, L, Pettersson, H.* Chem. Rev, 2010. **110**: p. 6595-6663.

[5]. Dillon, A., *Carbon nanotubes for photoconversion and electrical energy storage.* Chemical Reviews, 2010. **110**(11): p. 6856-6872.

[6]. Kondratenko, E.V., et al., *Status and perspectives of CO 2 conversion into fuels and chemicals by catalytic, photocatalytic and electrocatalytic processes.* Energy & environmental science, 2013. **6**(11): p. 3112-3135.

[7]. Christopher, K. and R. Dimitrios, *A review on exergy comparison of hydrogen production methods from renewable energy sources.* Energy & Environmental Science, 2012. **5**(5): p. 6640-6651.

[8]. Cook, T.R., et al., *Solar energy supply and storage for the legacy and nonlegacy worlds.* Chemical reviews, 2010. **110**(11): p. 6474-6502.

[9]. Yang, Z., et al., *Electrochemical energy storage for green grid.* Chemical reviews, 2011. **111**(5): p. 3577-3613.

[10]. Miller, J.R. and P. Simon, *Electrochemical capacitors for energy management.* Science, 2008. **321**(5889): p. 651-652.

[11]. Wang, H. and H. Dai, *Strongly coupled inorganic–nano-carbon hybrid materials for energy storage.* Chemical Society Reviews, 2013. **42**(7): p. 3088-3113.

[12]. Chu, A. and P. Braatz, *Comparison of commercial supercapacitors and high-power lithium-ion batteries for power-assist applications in hybrid electric vehicles: I. Initial characterization.* Journal of power sources, 2002. **112**(1): p. 236-246.

[13]. Pandolfo, T., et al., *Supercapacitors: Materials, Systems, and Applications.* General Properties of Electrochemical Capacitors, Wiley-VCH Verlag, Weinheim, Germany, 2013: p. 69e109.

[14]. Wang, F., et al., *Electrode materials for aqueous asymmetric supercapacitors.* Rsc Advances, 2013. **3**(32): p. 13059-13084.

[15]. Pell, W.G. and B.E. Conway, *Peculiarities and requirements of asymmetric capacitor devices based on combination of capacitor and battery-type electrodes.* Journal of Power Sources, 2004. **136**(2): p. 334-345.

[16]. Chen, P.-C., et al., *Preparation and characterization of flexible asymmetric supercapacitors based on transition-metal-oxide nanowire/single-walled carbon nanotube hybrid thin-film electrodes.* ACS nano, 2010. **4**(8): p. 4403-4411.

[17]. Cheng, Q., et al., *Graphene and nanostructured MnO2 composite electrodes for supercapacitors.* Carbon, 2011. **49**(9): p. 2917-2925.

[18]. Fan, Z., et al., *Asymmetric supercapacitors based on graphene/MnO2 and activated carbon nanofiber electrodes with high power and energy density.* Advanced Functional Materials, 2011. **21**(12): p. 2366-2375.

[19]. Aravindan, V., et al., *Insertion-type electrodes for nonaqueous Li-ion capacitors.* Chemical reviews, 2014. **114**(23): p. 11619-11635.

[20]. Qie, L., et al., *Synthesis of functionalized 3D hierarchical porous carbon for high-performance supercapacitors.* Energy & Environmental Science, 2013. **6**(8): p. 2497-2504.

[21]. Chen, P., et al., *Inkjet printing of single-walled carbon nanotube/RuO 2 nanowire supercapacitors on cloth fabrics and flexible substrates.* Nano Research, 2010. **3**(8): p. 594-603.

[22]. Park, M.S., et al., *A Novel Lithium-Doping Approach for an Advanced Lithium Ion Capacitor.* Advanced Energy Materials, 2011. **1**(6): p. 1002-1006.

[23]. Lam, L. and R. Louey, *Development of ultra-battery for hybrid-electric vehicle applications.* Journal of power sources, 2006. **158**(2): p. 1140-1148.

[24]. Frackowiak, E. and F. Beguin, *Carbon materials for the electrochemical storage of energy in capacitors.* Carbon, 2001. **39**(6): p. 937-950.

[25]. Deng, W., et al., *Potassium hydroxide activated and nitrogen doped graphene with enhanced supercapacitive behavior.* Science of Advanced Materials, 2018. **10**(7): p. 937-949.

[26]. Pandolfo, A. and A. Hollenkamp, *Carbon properties and their role in supercapacitors.* Journal of power sources, 2006. **157**(1): p. 11-27.

[27]. Ali, G.A., et al., *CaO impregnated highly porous honeycomb activated carbon from agriculture waste: symmetrical supercapacitor study.* Journal of materials science, 2019. **54**(1): p. 683-692.

[28]. Chen, M., et al., *Preparation of activated carbon from cotton stalk and its application in supercapacitor.* Journal of Solid State Electrochemistry, 2013. **17**(4): p. 1005-1012.

[29]. Subramanian, V., et al., *Supercapacitors from activated carbon derived from banana fibers.* The Journal of Physical Chemistry C, 2007. **111**(20): p. 7527-7531.

[30]. Hegde, G., et al., *Biowaste sago bark based catalyst free carbon nanospheres: waste to wealth approach.* ACS Sustainable Chemistry & Engineering, 2015. **3**(9): p. 2247-2253.

[31]. Ali, G.A., et al., *Carbon nanospheres derived from Lablab purpureus for high performance supercapacitor electrodes: a green approach.* Dalton Transactions, 2017. **46**(40): p. 14034-14044.

[32]. Ali, G.A.M., et al., *Superior supercapacitance behavior of oxygen self-doped carbon nanospheres: a conversion of Allium cepa peel to energy storage system.* Biomass Conversion and Biorefinery, 2019. DOI:10.1007/s13399-019-00520-

[33]. Wang, G., L. Zhang, and J. Zhang, *A review of electrode materials for electrochemical supercapacitors.* Chemical Society Reviews, 2012. **41**(2): p. 797-828.

[34]. Simon, P. and Y. Gogotsi, *Capacitive energy storage in nanostructured carbon–electrolyte systems.* Accounts of chemical research, 2012. **46**(5): p. 1094-1103.

[35]. Yan, J., et al., *Recent advances in design and fabrication of electrochemical supercapacitors with high energy densities.* Advanced Energy Materials, 2014. **4**(4): p. 1300816.

[36]. Natalia, M., Y. Sudhakar, and M. Selvakumar, *Activated carbon derived from natural sources and electrochemical capacitance of double layer capacitor.* 2013.

[37]. Leimkuehler, E.P., *Production, characterization, and applications of activated carbon*. 2010, University of Missouri--Columbia.

[38]. Dobashi, A., et al., *Preparation of activated carbon by KOH activation from amygdalus pedunculata shell and its application for electric double-layer capacitor.* Electrochemistry, 2015. **83**(5): p. 351-353.

[39]. Li, X., et al., *Fabrication of γ-MnS/rGO composite by facile one-pot solvothermal approach for supercapacitor applications.* Journal of Power Sources, 2015. **282**: p. 194-201.

[40]. Mohamed, S.G., I. Hussain, and J.-J. Shim, *One-step synthesis of hollow C-NiCo 2 S 4 nanostructures for high-performance supercapacitor electrodes.* Nanoscale, 2018. **10**(14): p. 6620-6628.

[41]. Wang, S., et al., *N-doped carbon spheres with hierarchical micropore-nanosheet networks for high performance supercapacitors.* Chemical Communications, 2014. **50**(81): p. 12091-12094.

[42]. Zhou, H., et al., *Transforming waste biomass with an intrinsically porous network structure into porous nitrogen-doped graphene for highly efficient oxygen reduction.* Physical Chemistry Chemical Physics, 2016. **18**(15): p. 10392-10399.

[43]. Wang, Y., et al., *Nitrogen-doped porous carbon monoliths from polyacrylonitrile (PAN) and carbon nanotubes as electrodes for supercapacitors.* Scientific reports, 2017. **7**: p. 40259.

[44]. Lin, G., et al., *KOH activation of biomass-derived nitrogen-doped carbons for supercapacitor and electrocatalytic oxygen reduction.* Electrochimica Acta, 2018. **261**: p. 49-57.

[45]. Yuan, J., et al., *Tuning the electrical and optical properties of graphene by ozone treatment for patterning monolithic transparent electrodes.* ACS nano, 2013. **7**(5): p. 4233-4241.

[46]. Pei, S., et al., *Direct reduction of graphene oxide films into highly conductive and flexible graphene films by hydrohalic acids.* Carbon, 2010. **48**(15): p. 4466-4474.

[47]. Geng, Z., et al., *Highly efficient dye adsorption and removal: a functional hybrid*

of reduced graphene oxide–Fe 3 O 4 nanoparticles as an easily regenerative adsorbent. Journal of Materials Chemistry, 2012. **22**(8): p. 3527-3535.

[48]. Aunkor, M., et al., *The green reduction of graphene oxide.* Rsc Advances, 2016. **6**(33): p. 27807-27828.

[49]. Zhang, S., et al., *Activated carbon with ultrahigh specific surface area synthesized from natural plant material for lithium–sulfur batteries.* Journal of Materials Chemistry A, 2014. **2**(38): p. 15889-15896.

[50]. Sing, K.S.W., *Reporting physisorption data for gas/solid systems with special reference to the determination of surface area and porosity (Provisional)*, in *Pure and Applied Chemistry*. 1982. p. 2201.

[51]. Ardizzone, S., G. Fregonara, and S. Trasatti, *"Inner" and "outer" active surface of RuO2 electrodes.* Electrochimica Acta, 1990. **35**(1): p. 263-267.

[52]. Ali, G.A., et al., *One-step electrosynthesis of MnO2/rGO nanocomposite and its enhanced electrochemical performance.* Ceramics International, 2018. **44**(7): p. 7799-7807.

[53]. Seo, M.-K. and S.-J. Park, *Electrochemical characteristics of activated carbon nanofiber electrodes for supercapacitors.* Materials Science and Engineering: B, 2009. **164**(2): p. 106-111.

[54]. Sui, L., et al., *Supercapacitive behavior of an asymmetric supercapacitor based on a Ni (OH) 2/XC-72 composite.* New Journal of Chemistry, 2015. **39**(12): p. 9363-9371.

[55]. Shao, Y., et al., *Design and Mechanisms of Asymmetric Supercapacitors.* Chemical Reviews, 2018. **118**(18): p. 9233-9280.

تحضير والسلوك الكهروكيميائي للكربون المنشط من قشور ثمرة الرمان كمواد لتخزين الطاقة

منى محمود مراد[1] ، سيد يحي عطية[2] ، سعد محمد جمعه[2] ، مروة محرم[3] ،
رباب محمد ابو شهبه[1] ، محمد محمود رشاد[3]

1- قسم الكيمياء – كلية العلوم فرع البنات جامعة الازهر
2- قسم كيمياء الفلزات – معهد الدراسات المعدنية بالتبين
3- مركز بحوث الفلزات بالتبين

الملخص العربي

هذا البحث يقوم على اساس دراسة السلوك الكهروكيميائى للكربون النشط المحضر من المخلفات البيئية والاستفاده منها مثل قشور ثمره الرمان التى تم تجميعها وتجفيفها وعمل خطوه الحرق لقشور الرمان ثم بعد ذلك عمل تنشيط للماده المحضرة بهيدروكسيد البوتاسيوم عند درجات حراره مختلفة ومن ثم نقوم بدراسة كافة التوصيفات لها مثل قياس مساحة السطح والتى تمثل 3128.86 متر مربع لكل جرام، وقد تبين من خلال نتائج السلوك الكهروكيميائى ان الكربون النشط المحضر يعطى قيمة للسعة الكهربية تبلغ 126 فاراد لكل جرام عند تيار كهربى نصف امبير لكل جرام، وتبلغ نسبة الاحتفاظية للسعة الكهربية بعد عدد 2000 من الدورات الكهربية حوالى 137%عند تيار كهربى 2 امبير وعند عمل محاكاة معملية للكربون النشط المحضر واستخدامه كمكثف فائق وجد ان قيمة الطاقة النوعية هى 4.58 وات ساعة لكل جرام وقيمه قدرة نوعية 244 وات لكل جرام ونسبة الاحتفاظية للسعة الكهربية حوالى 66% عند تيار كهربى 2 امبير لكل جرام، ومن هذه النتائج والقيم يمكن اعتبار الكربون النشط احد المواد الناجحة والبسيطة التى يمكن استخدامها كمكثف فائق لتخزين الطاقة لحين الحاجه اليها